LA-UR- 97-2949

CONF-971157--

Los Alamos National Laboratory is operated by the University of California for the United States Department of Energy under contract W-7405-ENG-36.

TITLE: FLOW STRUCTURE IN A RAYLEIGH-BENARD CELL UPON IMPULSIVE SPIN-UP

AUTHOR(S): P. Vorobieff, CNLS, DX, MST, and T-Division
R. E. Ecke, MST

SUBMITTED TO 1997 ASME Annual Meeting Proceedings

Los Alamos

Los Alamos National Laboratory
Los Alamos, New Mexico 87545

FORM NO. 836 R4
ST. NO. 2629 5/81

DISCLAIMER

Flow structure in a Rayleigh-Bénard cell upon impulsive spin-up

P. Vorobieff and R.E. Ecke
Center for Nonlinear Studies and
Condensed Matter and Thermal Physics Group
Los Alamos National Laboratory
Los Alamos, NM 87545, USA

Abstract

We investigate convection in a cylindrical Rayleigh-Bénard cell with radius-to-height ratio $\Gamma = 1/2$. The cell is subjected to impulsive spin-up about its vertical axis. We use TLC (thermochromic liquid crystal) for temperature field measurements and PIV (particle image velocimetry) for the velocity reconstruction of the transition in the range of Rayleigh numbers R from 5×10^7 to 5×10^8 and Taylor numbers Ta from 0 up to 2.4×10^{10}. The initial (at rest) and the final (in steady rotation) states of the system are those of chaotic turbulent convection. The most persistent transient feature emerging is a sharply defined ringlike pattern or concentric patterns characterized by a decrease in temperature, axial velocity directed downward and high azimuthal shear. The latter leads to formation of an azimuthally regular structure of Kelvin-Helmholz vortices. During the next stage of the transition, the vortical structure loses azimuthal regularity and the pattern characteristic of turbulent rotating convection forms.

1. Introduction

Issues related to Rayleigh-Bénard convection have received considerable attention of researchers in the recent years, because of the importance of the phenomenon for a very wide range of applications – from astrophysics to engineering, and because it provides a convenient model problem for investigations of transition to turbulence. A fluid layer of height d heated from below and cooled from above remains stable and transmits heat by thermal diffusion only if the temperature difference across the layer ΔT does not exceed a critical value ΔT_c. At $\Delta T > \Delta T_c$, the buoyancy-driven Rayleigh-Bénard convection takes place in the layer, and heat is transported through it by a combination of diffusion and advection. The dimensionless parameters that govern the state of the flow in the simplest case of Rayleigh-Bénard convection are the Rayleigh number R, representing the amount of potential energy in the fluid, and the Prandtl numer σ determined by the properties of the fluid:

$$R = \frac{\alpha g \Delta T d^3}{\nu\kappa}, \quad \sigma = \frac{\nu}{\kappa}, \tag{1}$$

where α is the coefficient of thermal expansion, g is the acceleration of gravity, ν is the kinematic viscosity of the fluid, and κ is the fluid coefficient of thermal diffusivity. Another dimensionless parameter of importance is the aspect ratio $\Gamma = r_0/d$ between the vertical and characteristic lateral dimensions (the latter being, for instance, the radius of a cylindrical convection cell r_0).

The linear stability of the problem has been thoroughly investigated by Chandrasekhar[1]. At Rayleigh numbers $R \sim 4\times10^7$ and higher[2], the convection is characterized by thermal plumes being responsible for the general character of the flow. This state of convection is known as 'hard turbulence.' Convective heat transport is controlled by two sharp thermal boundary layers[3], and the scaling theory of Shraiman and Siggia[4] suggests that the interaction of the shear flow away from the boundaries with the thermal boundary layers is responsible for the heat transport scaling observed in experiments on helium gas[2].

The above is a very brief outline of the general problem of Rayleigh-Bénard convection. In particular, Rayleigh-Bénard convection in a rotating reference frame, representing the characteristic feature of many problems in diverse areas such as astrophysics, geophysics and engineering, has been the subject of numerous studies. Rotation adds the influence of Coriolis force and centrifugal effects to the problem, the strength of the Coriolis force in the dimensionless form represented by the dimensionless rotation rate, $\Omega = \Omega_D d^2/\nu$, where Ω_d is the angular rotation rate about the vertical axis.

The linear stability analysis for rotating convection was carried out by Chandrasekhar[5], and since the first experimental work of Nakagawa and Frenzen[6], there have been many investigations of rotating convection, most of which are reviewed by Boubnov and Golitsyn[7]. In rotating turbulent convection, the main flow feature is the presence of vortices (plumes) with cold downwelling cores (cyclonic) and hot upwelling cores (anticyclonic), the number of which grows with the rotation rate. Several authors have reported formation of regular structures in the flow if the rotating convection cell is subjected to rapid changes in either R (Dikarev[8], Zhong *et al.*[9]) or Ω (Boubnov and Golitsyn[10]). Formation of axially regular features upon rapid spin-up from rest of the convection cell is the subject of the current study. We present time sequences of instantaneous tempera-

ture maps and velocity fields in the plane adjacent to the top of the cell that show the presence of rings of downwelling cold flow characterized by an abrupt change in azimuthal velocity. As our previous investigation shows[11], the number of such rings grows with the final rotation rate and also depends on the Rayleigh number. As shear develops across the rings, Kelvin-Helmholz instability causes roll-up of vortices, leading to destruction of the rings.

2. Experimental Details

A cylindrical Plexiglas cell of radius $r_0 = 6.35$ cm and height $d = 12.7$ cm is placed on a rotating table. The bottom boundary of the cell is an anodized aluminium plate attached to a disk-shaped heating element with the radius equal to that of the cell. The top boundary of the cell is a transparent sapphire window separating the cell from a cooling manifold through which temperature-controlled water is circulated. Thus the top boundary of the cell is maintained at constant temperature T_t, while at the bottom boundary the heat flux into the cell is maintained constant, resulting in constant bottom temperature T_b in steady rotating convection. A lighting system producing a thin (~ 3 mm) sheet of white light can illuminate horizontal sections of the cell, and a color digital video camera is positioned on the rotating table above the cell. Fig. 1 presents a schematic view of the cell.

In the plane of the light sheet, instantaneous fields of temperature and horizontal velocity can be acquired. For temperature field acquisition, the flow is seeded with 5-μm microcapsules with thermochromic liquid crystals (TLC). TLCs selectively reflect incident white light – within the range of their color play, they change the wavelength of the color they reflect monotonically with temperature, red corresponding to the lower end of the color play range, and blue to the upper. Thus color digital images of the light sheet illuminating the flow in the cell seeded with TLC microcapsules can be converted to temperature maps by extracting their hue component and mapping the hue of each pixel to temperature. For velocity acquisition, we seed the flow with neutrally buoyant polystyrene microspheres and apply the standard particle image velocimetry (PIV) technique to recover velocities from microsphere displacements between consecutive frames of digital video images of the flow. Details of TLC temperature mapping and PIV velocity acquisition in application to this problem, as well as accuracy of both techniques, are discussed elsewhere[11]. The error in temperature reconstruction appears not to exceed 0.11^O C. We used a digital PIV system capable of acquiring 30 640 by 480 frames per second. The spatial resolution of this system limited the size of the grid for the velocity data recovered to 27 by 27 – sufficient to resolve the larger-scale features of the flow with 99% accuracy, but unable to recover information about features of sizes 0.5 cm and smaller.

3. Observations

A sequence of velocity/temperature maps characteristic of the flow evolution during spin-up is presented in Fig. 2. The value of the Rayleigh number ($R = 2 \times 10^8$) is dictated by the color play range of the TLC – 3.6 ^{O}C, and the cell undergoes impulsive spin-up to $\Omega = 1.9 \times 10^{-1}$. Velocity temperature were acquired in two separate runs of the experiment under identical conditions, but with different seeding particles. In both runs, the horizontal light sheet was positioned adjacent to the top boundary of the cell. The time in Fig. 2 has been nondimensionalized with Ekman spin-up time $\tau_E = d/\sqrt{\nu\Omega_D}$ – the characteristic time scale for the problem of spin-up to rotation rate Ω without convection.

Immediately before spin-up, Fig. 2 $t/\tau_E = 0$, the flow is dominated by upwelling plumes of hot material separated with elongated zones of cool downwelling flow clearly visible in the temperature map. The characteristic velocity due to turbulent convection before spin-up is on the order of mm/s. Upon spin-up ($t/\tau_E = 0.03$), the azimuthal velocity imparted to the water in the cell in the layer adjacent to the horizontal walls is on the order of $\Omega_D r_0 = 58$ mm/s. In the rotating reference frame, this corresponds to the core of the cell being in solid-body rotation with azimuthal velocity growing linearly with distance from the axis of the cell and then entering the area near the wall and dropping to zero. The velocity distribution closely matches that predicted and measured by Weidman[12,13] for impulsive spin-up of a cylindrical cell without convection. It is also noteworthy that at the early stages of spin-up all the structures in the temperature field near the top of the cell are destroyed. As the flow evolves, colder fluid accumulates at the outer perimeter of the cell due to centrifugal effects. At dimensionless time $t/\tau_E \sim 0.4$, a thin cold ring forms at a radius $r_r \simeq 3/4\ r_0$. Formation of this ring is also associated with changes in the velocity field: the ring is associated with a a local minimum in the velocity profile (Fig. 2, $t/\tau_E = 0.53$). This feature of the velocity field is specific for spin-up with convection – neither Weidman's solution[12] nor the experiments[13,11] produce velocity profiles with local minima for the non-convective spin-up problem. The next stage of the evolution is the roll-up of Kelvin-Helmholz vortices in the ring due to az-

imuthal shear ($t/\tau_E = 0.98$). After the formation of the cyclonic vortices, the flow loses its azimuthal regularity, resulting in the irregular vortex pattern characteristic of rotating convection at high Rayleigh numbers.

As reported in our previous work[11], this pattern of flow evolution is observed within a considerable range of the domain of the parameter space $R - \Omega$ we investigated. At a fixed Rayleigh number, there exists an interval of rotation rates at which one ring forms, with its radius showing a remarkably weak dependence on either R or Ω and remaining close to $r_r \simeq 3/4\ r_0$. Spin-up to low Ω does not lead to ring formation, while at Ω exceeding a certain critical value for each R we observe formation of two rings, the inner still at $r_r \simeq 3/4\ r_0$ and the outer at $r_r \simeq 0.94\ r_0$. Further increase in Ω leads to formation of three rings during spin-up, the third and innermost ring having the radius $r_r \simeq 0.56\ r_0$. Again, the radii of the rings show only a weak dependence on R and Ω. Figure 3 shows the time sequence of temperature maps for spin-up to $\Omega = 7.2 \times 10^4$ at $R = 2 \times 10^8$. The first image, with spin-up imminent, shows a typical temperature map of non-rotating convection, with cooled material downflow areas forming elongated zones between the upwelling plumes. The following two images, acquired shortly after the impulsive spin-up of the cell, show the temperature maps prior to the formation of the ring. At dimensionless time t/τ_E close to 1, one can observe the outer cold ring forming near the vertical wall. The ring at $r_r \simeq 3/4\ r_0$ forms next, at dimensionless time 1.67, and at $t/\tau_E \sim 2$ vortices begin to roll up in the outer two rings and the innermost third ring becomes visible. Subsequent evolution produces a staggered structure of cyclonic and anticyclonic vortices in the place of the two outer rings coexisting with the innermost ring at $t/\tau_E = 2.37$. At later times, the inner ring is likewise destroyed by vortex roll-up, and the structure of the flow loses its regularity and eventually evolves to a steady rotating convection pattern.

The rotation rates characterizing the transition from the flow pattern without rings to the one-ring pattern, from the one-ring pattern to the two-ring pattern, etc. grow with the Rayleigh number[11].

4. Conclusions

For the impulsive spin-up of a Rayleigh-Bénard cell, we produce time sequences of instantaneous horizontal velocity and temperature maps in the plane adjacent to the top cooled surface of the cell. The most prominent features of the flow morphology observed during the spin-up are axisymmetric ring-shaped zones of downwelling flow characterized by a local drop in temperature and azimuthal velocity. While the number of the rings increases with the increase in the final rotation rate, the charactriistic radii of the rings do not show a strong dependence on either R or Ω.

The flow evolution during spin-up can be divided into three stages. First, the flow structures typical of the non-rotating convection are destroyed by the acceleration of the cell, and a relatively uniform temperature field forms near the top boundary. At this stage, one can also observe accumulation of the cooler fluid near the vertical wall. During the first stage, the velocity distribution is consistent with that calculated and measured for the spin-up of a cylindrical cell without convection. In the second stage, cold downwelling ring(s) form. Azimuthal velocity undergoes sharp changes in the rings, and the velocity profiles no longer resemble ones typical for the no-convection spin-up. Finally, shear in the rings leads to roll-up of Kelvin-Helmholz vortices.

5. Acknowledgments

We gratefully acknowledge the support of the U.S. Department of Energy for our research.

1. S. Chandrasekhar, "Hydrodynamic and Hydromagnetic Stability," Oxford University Press (1961).
2. F. Heslot, B. Castaing and A. Libchaber, "Transitions to turbulence in helium gas," *Phys.Rev. A*36, 5870 (1987).
3. E.D. Siggia, "High Rayleigh number convection," *Annu. Rev. Fluid Mech.* **26**, 137 (1994).
4. B.I. Shraiman and E.D. Siggia, "Heat-transport in high-Rayleigh-number convection," *Phys. Rev. A* **42**(No. 6). 3650 (1990).
5. S. Chandrasekhar, "The instability of a layer of a fluid heated from below and subject to Coriolis forces," *Proc. R. Soc. Lond.* A **217**, 306 (1953).
6. Y. Nakagawa and P. Frenzen, "A theoretical and experimental study of cellular convection in rotating fluids," *Tellus* A **7**, 1 (1955).
7. B.M Boubnov and G.S. Golitsyn, "Convection in rotating fluids," Dordrecht; Boston, Kluwer Academic (1995).
8. S.N. Dikarev, "On the influence of rotation on the convection structure in a deep homogeneous fluids," *Dokl. Akad. Nauk SSSR* **273**, 718 (1983) (in Russian).
9. F. Zhong, R.E. Ecke and V. Steinberg, "Rotating Rayleigh-Bénard convection: asymmetric modes and vortex states," *J. Fluid Mech.* **249**, 135 (1993).
10. B.M. Boubnov and G.S. Golitsyn, "Experimental study

of convective structures in rotating fluids," *J. Fluid Mech.* **23**, 503 (1986).

11. P. Vorobieff and R.E. Ecke, "Transient states during spin-up of a Rayleigh-Bénard cell," submitted to *Phys. Fluids*, July 1997.
12. P.D. Weidman, "On the spin-up and spin-down of a rotating fluid. Part 1. Extending the Wedemeyer model," *J. Fluid Mech.* **77**, 685 (1976).
13. P.D. Weidman, "On the spin-up and spin-down of a rotating fluid. Part 2. Measurements and stability," *J. Fluid Mech.* **77**, 709 (1976).

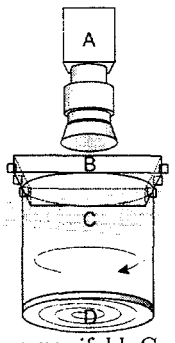

Fig. 1. Experimental setup. A – camera, B – cooling manifold, C – illuminated section of the cell, D – bottom plate with heater.

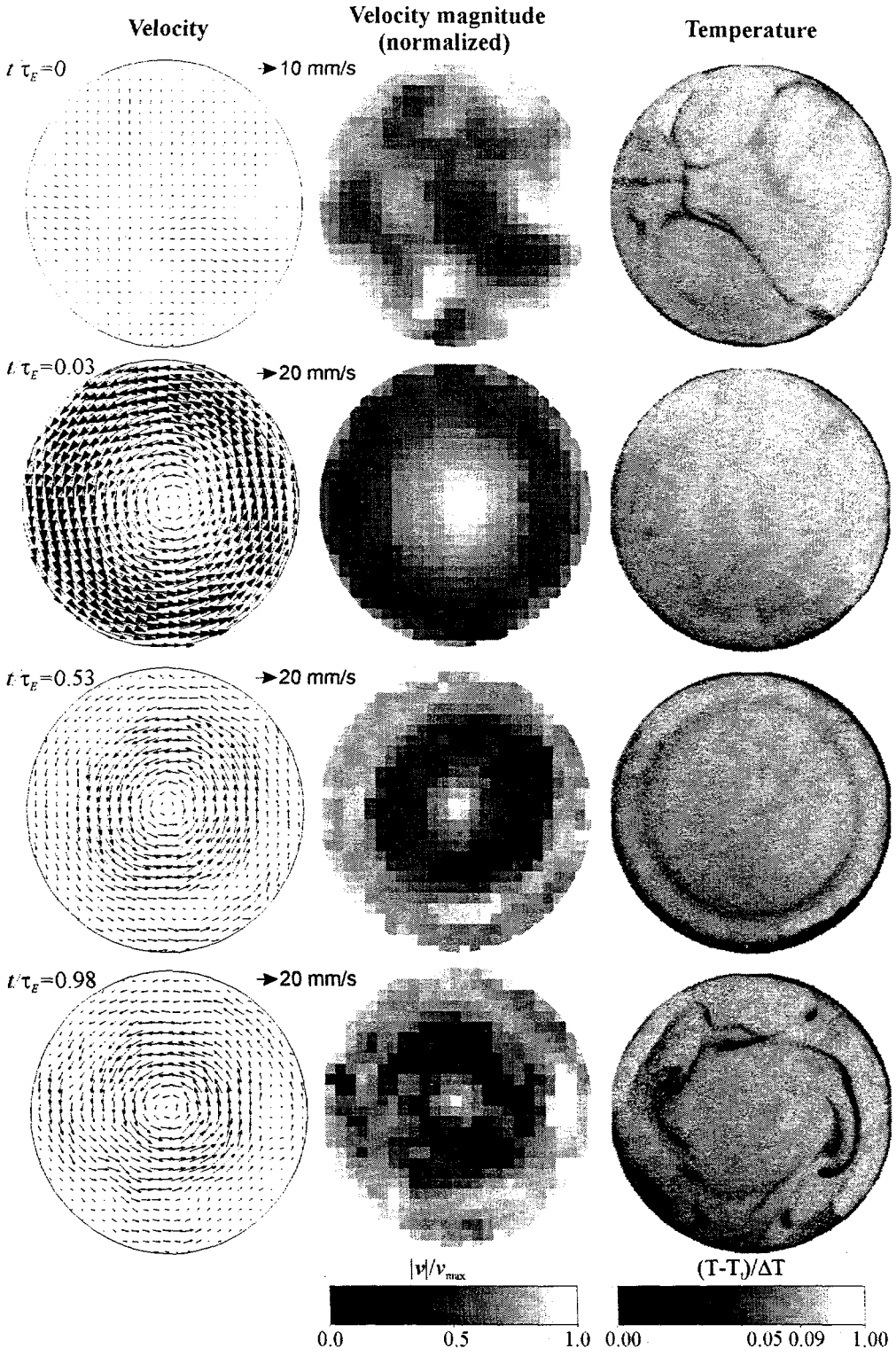

Fig. 2. Maps of instantaneous horizontal velocity (left column, velocity scale indicated for each map), velocity magnitude (center column, normalized by maximum velocity for each map) and temperature (right column) of spin-up to $\Omega = 1.9 \times 10^{-4}$ at $R = 2 \times 10^8$. Dimensionless times are indicated in the figure.

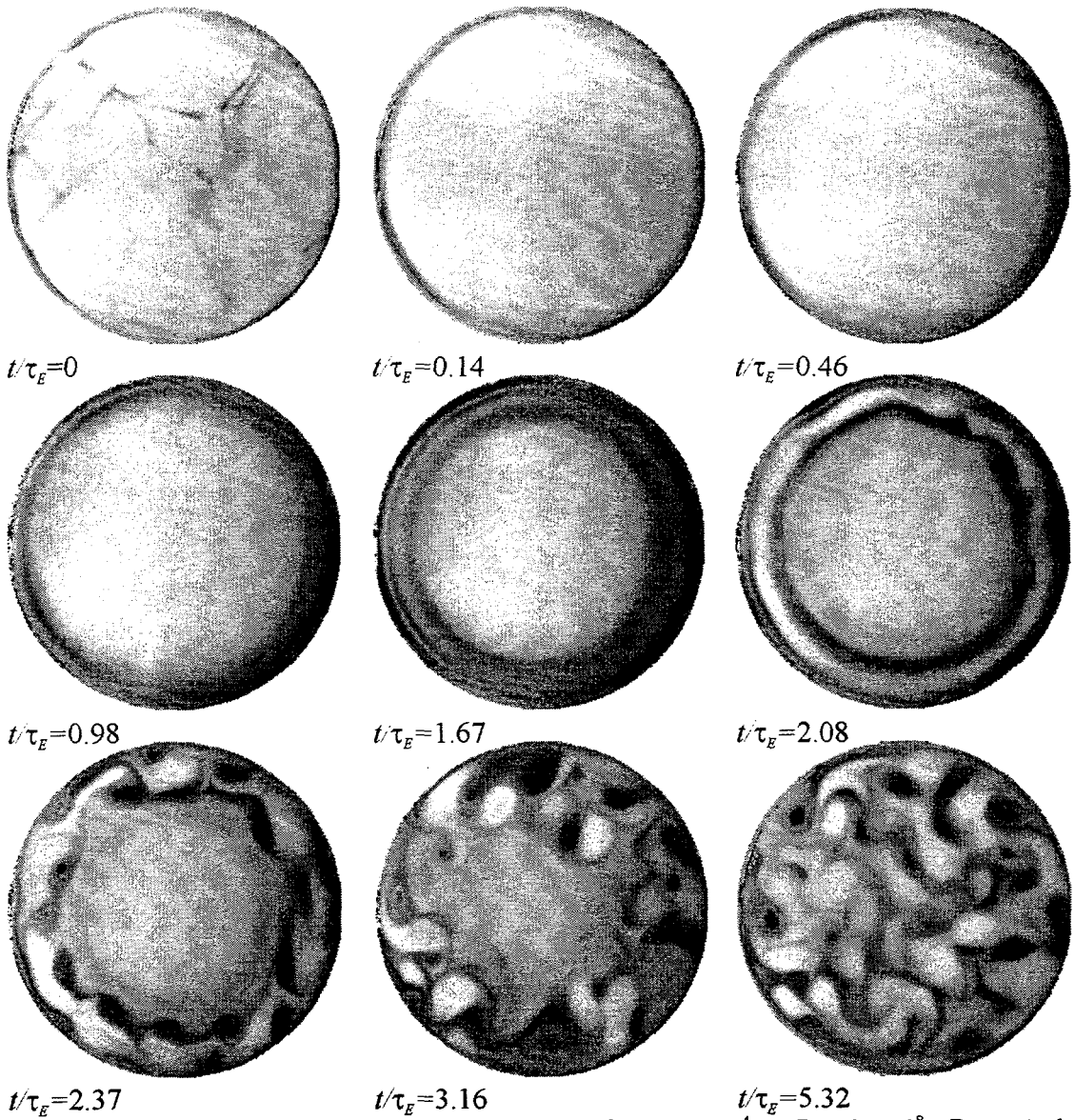

Fig. 3. Instantaneous TLC temperature maps of spin-up to $\Omega = 7.2 \times 10^4$ at $R = 2 \times 10^8$. Dimensionless times are indicated in the figure.